Modeling L1-GPS Errors for an Enhanced Data Fusion with Lane Marking Maps for Road Automated Vehicles

Zui Tao, Philippe Bonnifait

MODELING L1-GPS ERRORS FOR AN ENHANCED DATA FUSION WITH LANE MARKING MAPS FOR ROAD AUTOMATED VEHICLES

Zui Tao, Philippe Bonnifait

Sorbonne universités, Université de technologie de Compiègne, CNRS, Heudiasyc UMR 7253, CS 60 319, 60 203 Compiègne cedex
Email: zui.tao@hds.utc.fr
Email: philippe.bonnifait@hds.utc.fr

ABSTRACT: This paper describes a method which models the time correlation errors of a standalone L1-GPS receiver by integrating front-view camera measurements map-matched with a lane marking map. An identification method of the parameters of the shaping model is presented and evaluated with real data. The observability of the augmented state vector is demonstrated according to an algebraic definition. A positioning solver based on extended Kalman filtering with measured input is developed in the local ENU (East-North-Up) frame. This formulation allows including efficiently speed sensors in a dead-reckoned way. Outdoor experiments results carried out with a ground truth system are used to illustrate the performance of the proposed method.

1 INTRODUCTION

Estimating the pose in real-time is a primary function for road automated vehicles. Recently, highly accurate digital maps have become key components for autonomous vehicle navigation and can enhance the positioning performance [1][2][3]. In this paper, we propose to use a lane marking map of the navigation area with centimetre-level precision. The map consists of two-lane roadways with dashed lane markings in the centre of the road and solid lane markings on the both sides of the road. Lane marking is expressed by polylines in a local frame near the navigation area. In order to exploit this lane marking map, we have integrated a camera from the Lane Departing Warning Systems of the experimental vehicle. The camera's lane marking detection module is able to measure the lateral distance between the detected lane marking and the vehicle in the camera frame. The camera can also identify the type of the detected lane markings (solid, dashed and road edge). Since the camera gives relative measurements, the next step is to relate the measures with the vehicle's state. For this, we have proposed a refined camera observation model which express camera measurement by a function of the state vector and the parameters of the detected lane marking [4]. So a data association process is necessary to associate a camera measurement with a certain lane marking segment in the map database. It is similar to a map matching process. The difference is that the map matching process can introduce a non-zero mean errors by simply projecting the vehicle position onto a segment which usually represents the road centreline. However, the camera has limitations. For example, there is no lane markings in some parts of the navigation area and the camera often fails to detect lane marking at cross-roads. If the uncertainty domain grows too quickly during these times, it can be very challenging to distinguish different lanes when the camera retrieves measurements. Therefore Dead-Reckoning (DR) sensors are integrated to increase the performance particularly in terms of availability. We demonstrate the observability of the gyro bias thanks to the camera observation. It is important to note that the camera observation can only improve the positioning in lateral direction for a given moment, although the longitudinal accuracy is also improved if the road changes direction. GPS is very useful to compensate DR's long-term drift and it is mandatory for a cold start initialization of the localization system. However the L1-GPS positioning errors are not white and can be affected by strong biases, which are mainly due to atmosphere propagation delays, multi-path and real-time orbit errors, particularly in urban area.

In this paper, we study GPS biases shaping models that are used in a filter by augmenting the state vector. The GPS errors are studied thanks to the use of a high-end localization system with centimetre-level accuracy. Autocorrelations of different sequences are analysed to find repeatable behaviour supposing that the bias is stationary (GPS measures with abrupt bias changing according to multi-path is supposed to be rejected by the localization solver). The bias is modeled by an autoregressive model. Parameters identification methods are discussed for integrating the shaping filter into the localization solver. The observability of GPS biases being not obvious, one of our contribution is the demonstration of the observability of the augmented state vector, which contains the pose of the vehicle, a gyro bias and GPS errors, according to an algebraic definition.

The remainder is organized as follows. Section 2 introduces the GPS error modeling. Section 3 describes the system modeling and demonstrates the observability of the state vector. Outdoor experimental results are reported in Section 4. Section 5 concludes the paper.

2 GPS ERROR MODELS FOR LOOSELY COUPLING DATA FUSION

GPS is mandatory for a cold start initialization of the system. Moreover, GPS information has to be used as much as possible as long as it is consistent with the pose estimate.

Indeed, when there is no lane marking in a navigation area or when the camera fails to detect lane markings at cross-roads for instance, GPS is useful to improve the accuracy of the pose information and compensate Dead-Reckoning errors. Moreover, since the camera observations provide only lateral correction, if the vehicle travels in a long straight road, the longitudinal drift of a map-aided dead-reckoned estimate can become significant. The GPS information can again be used to correct the longitudinal drift.

In order to do the data fusion of GPS fixes, we propose to estimate their positioning errors by augmenting the state vector. In this section, the errors on GPS fixes are described and modelled with shaping filters.

2.1 Typical GPS errors

As well known, loosely coupling L1-GPS with other sensors is a challenging task since GPS positioning errors are not white and can be affected by strong biases (due to atmosphere propagation delays) and multipath, particularly in urban areas. Fig. 1 illustrates these issues on a real test with a ground truth system: positioning errors can reach several meters, they are strongly correlated and can have jumps during short times. The solution that we propose is to model the correlation to compensate the biases and to reject fixes that are due essentially to multipath.

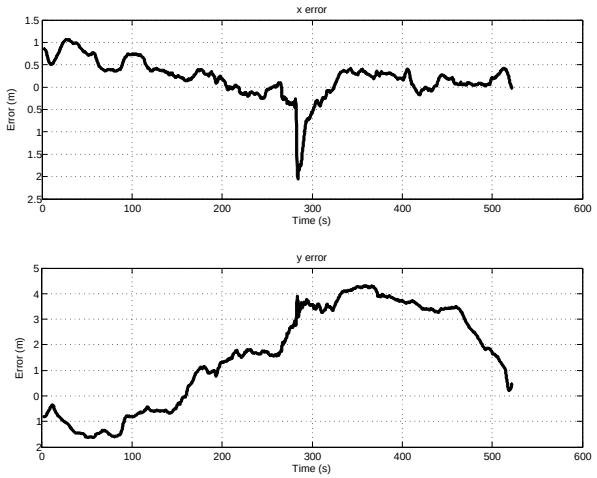

Fig. 1. Errors of L1-GPS solutions in the local navigation frame

2.2 GPS error models

Autocorrelations of 3 different sequences of a L1-GPS receiver (1000 samples each at 5 Hz) are shown in Fig. 2. As the shape is clearly different from a Delta-Dirac at zero, errors are coloured. Moreover, for short correlation time (smaller than 30 seconds), the different curves superimpose quite well which indicates a quite repeatable behaviour which can be modeled.

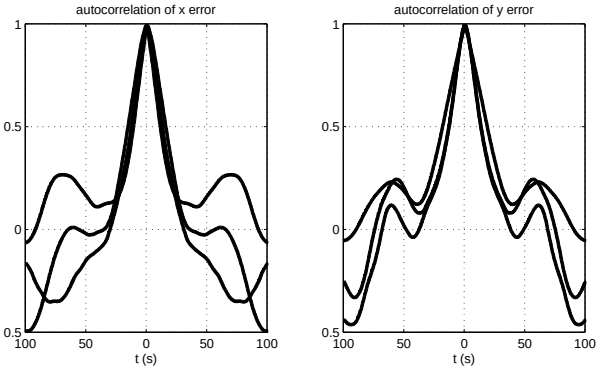

Fig. 2. Autocorrelation of three different sequences

Therefore, each L1-GPS error can be modelled by a zero-mean white noise passing through a shaping filter to yield an output statistically similar to the error under consideration. Let $[\varepsilon_x\ \varepsilon_y]^T$ denotes the vector of GPS errors. The problem is to find a structure for the filter and then to estimate its parameters and the variance of the driving noise. Moreover, GPS errors are quite non-stationary (even if they have a correlation from day to day at a given place since the repetition of the satellites geometry is approximately 24 hours). So, the error model has to be quite robust with respect to this non-stationarity.

2.2.1 Autoregressive (AR) process for modelling GPS random errors

An AR model is a representation of a type of random process. The name autoregressive comes from the fact that each signal sample is regressed on the previous values of itself. The AR process can be described using a pole-zero transfer system ($H(z)$) as follows:

$$H(z) = \frac{O(z)}{I(z)} = \frac{\beta_0}{1+\sum_{n=1}^{p} a_n z^{-n}} \tag{1}$$

where $I(z)$ is the z-transform of the input I_k, $O(z)$ is the z-transform of the output O_k. ${\beta_0}^2$ represents the estimated variance of the white noise input to the AR model; p is the AR order.

Applying the inverse z-transform to (1), the AR sequential process in the time domain is given by:

$$O_k = -\sum_{n=1}^{p} a_n O_{k-n} + \beta_0 I_k \tag{2}$$

In [4], the AR processes are used to model the randomness of inertial sensor measurements. The residual random error component is modelled as a zero-mean white noise passing through a shaping filter to yield an output with an adequate time-correlation. Here, we suggest using the same AR structure to model GPS random errors. So, in our case, (2) becomes:

$$\begin{cases} \varepsilon_{x,k} = -\sum_{n=1}^{p} a_{x,n}\varepsilon_{x,k-n} + \omega_{x,k} \\ \varepsilon_{y,k} = -\sum_{n=1}^{p} a_{y,n}\varepsilon_{y,k-n} + \omega_{y,k} \end{cases} \tag{3}$$

where ε_x and ε_y are the non-white errors on GPS position fixes; ω_x and ω_y are the input white noises. The following section discusses the determination of the AR model coefficients ($a_{x,n}$ and $a_{y,n}$), the input white noises and the AR order p.

2.2.2 AR coefficients and noises estimation

There are different methods to estimate the parameters by fitting an AR model to the input data. In [5], three different methods for the estimation of AR model parameters are investigated: the Yule-Walker method, the covariance method and the Burg's method. The Yule-Walker method determines first the sample autocorrelation sequence of the input signal (GPS residual errors in our case). Then the AR model parameters are optimally computed by solving a set of linear normal equations in a least-square sense. However, the Yule-walker method performs adequately only for very long data records [6] and it may introduce a large bias in the estimated AR coefficients, since it does not guarantee a stable solution. The covariance method is similar to the Yule-Walker method in minimizing the prediction error in the least-squares sense. Burg's method was introduced to overcome most of the drawbacks of the other modelling techniques by providing both stable and high resolution, especially for short data records [7]. Burg's method tries to make the maximum use of the data by defining both a forward and a backward prediction error terms. For these reasons, the Burg's method is adopted here to estimate the AR coefficients and the variance of the input white noises of the shaping filter.

2.2.3 Discussion on the AR order

In this section, the choice of the order of the AR model is discussed. Considering the complexity and time efficiency of integrating the AR model into a shaping filter, the study is limited up to order 2.

Eight tests have been made to collect the GPS data for a vehicle driving in normal conditions. The GPS errors are calculated in comparison to a ground truth system with centimetre-level accuracy. The AR parameters are calculated with Burg's method.

Fig. 3 shows the variation of the AR1 and AR2 coefficients respectively. One can notice that the biggest variation of the AR1 coefficients is not more than 0.05%. However, the variation of AR2 coefficients reaches nearly 40%. Even if the

sequences, which we have used to identify the parameters, are probably too short to estimate the AR2 parameters adequately, it is clear that the stability of an AR1 model is better. Our strategy is so to use a lower order filter but more robust to the non-stationarity, which means in other words an AR process of order 1.

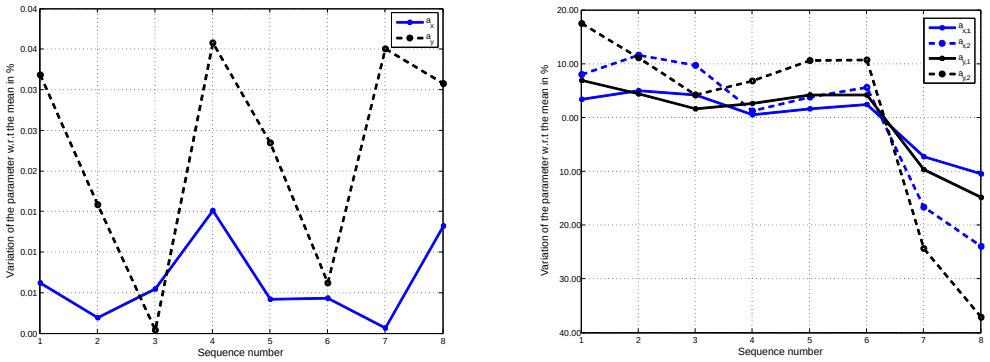

(a) AR1 coefficients variation (b) AR2 coefficients variation

Fig. 3. AR coefficients estimation variation (Burg's method)

In order to validate the shaping filter, we reverse it in offline processing by using the following discrete time difference system:

$$\begin{cases} \omega_{x,k} = \varepsilon_{x,k} + a_x \varepsilon_{x,k-1} \\ \omega_{y,k} = \varepsilon_{y,k} + a_y \varepsilon_{y,k-1} \end{cases} \tag{4}$$

The autocorrelations of $\omega_{x,k}$ and $\omega_{y,k}$ are given in Fig.4 (red ones), which approximate quite well a Delta-Dirac. Thus, we can conclude that these signals are white noise sequences, and the AR1 model defined by (4) is a good shaping filter.

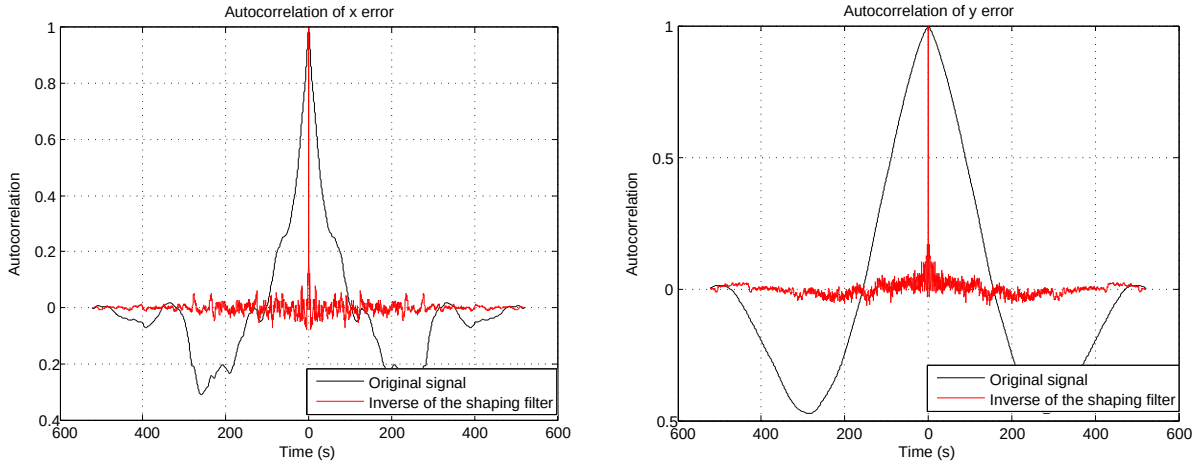

Fig. 4. Autocorrelation of experimental signal and the inverse of the shaping filter

3 SYSTEM MODELING AND STRUCTURAL PROPERTIES ANALYSIS

In section 2, the GPS positioning errors have been modelled by a first order autoregressive model. A classical way to handle this kind of modelling is to augment the state vector with a shaping filter [8]. The state vector becomes:

$$X = [x, y, \psi, \varepsilon_\omega, \varepsilon_x, \varepsilon_y]^T \tag{5}$$

The state evolution model is:

$$\begin{cases} \dot{x} = v \cdot \cos\psi \\ \dot{y} = v \cdot \sin\psi \\ \dot{\psi} = \omega - \varepsilon_\omega \\ \dot{\varepsilon_\omega} = 0 \\ \dot{\varepsilon_x} = -\varepsilon_x/\tau_x \\ \dot{\varepsilon_y} = -\varepsilon_y/\tau_y \end{cases} \tag{6}$$

where (x, y, ψ) is the vehicle 2D pose; ε_ω is the bias of gyro measurements; τ_x and τ_y are the time constants of the shaping filter.

Since GPS component errors are additive, their observability is not obvious. In this section, we prove the observability of the state vector.

Theorem: (cf. [9]) A state element is observable with respect to $Z = \{Y, U\}$, if and only if it can be expressed by an algebraic function of component of Z and a finite number of their derivatives. Y is the measurement vector and U is the input vector.

In [9], this algebraic definition of observability is used to prove that angular measurements provided by a camera are enough to perform localization in challenging conditions. For nonlinear systems, this definition of observability is more powerful than geometrical concepts based on Lie derivatives [10] since it provides necessary and sufficient conditions [11].

In [4], we compared three different GPS error models, and the observability was proved in a simplified case: frame-to-frame transformation is done by choosing the origin point of working frame on the lane marking with its x-axis parallel with the lane marking. The longitudinal errors are observable as soon as the vehicle trajectory presents changes of direction. However, if the vehicle travels along a long straight road and the GPS longitudinal error property changes with time, the observability is not guaranteed. Here, we demonstrate the observability in a fixed frame in which GPS errors on x and y are modelled as autoregressive processes.

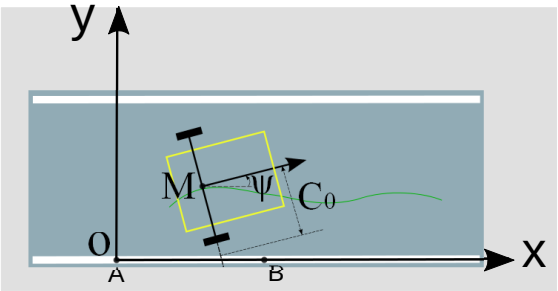

Fig. 5. Simplified camera observation model

In order to prove the observability of GPS measurement errors, let us simplify the state-space model by supposing that camera and the GPS antenna are coinciding with point M (Fig. 5). As in [4], a frame-to-frame transformation is performed to simplify the camera observation model (cf. [12]) by choosing the origin of the working frame as point A of the detected lane marking with its x-axis parallel to the lane marking. Consequently, camera and GPS observation model are simplified to:

$$C_0 = y/\cos\psi \tag{7}$$

and

$$\begin{cases} x_{GPS} = x + \varepsilon_x \\ y_{GPS} = y + \varepsilon_y \end{cases} \tag{8}$$

We have $Y = [x_{GPS}, y_{GPS}, C_0]$ and $U = [v, \omega]$ to analyze the observability of the state vector in the algebraic framework.

3.1 Observability of the vehicle heading ψ and gyro bias ε_ω

By taking the derivative of (7), we have:

$$\dot{y} = \dot{C_0} \cdot \cos\psi - C_0 \cdot \dot{\psi} \cdot \sin\psi \tag{9}$$

By plugging $\dot{y} = v \cdot \sin\psi$ and $\dot{\psi} = \omega - \varepsilon_\omega$ into (9):

$$v \cdot \sin\psi = \dot{C}_0 \cdot \cos\psi - C_0(\omega - \varepsilon_\omega)\sin\psi \tag{10}$$

By taking the derivative of (10), we have:

$$[\dot{v} + 2\dot{C}_0(\omega - \varepsilon_\omega) + \dot{\omega} \cdot C_0]\sin\psi = [\ddot{C}_0 - C_0(\omega - \varepsilon_\omega)^2 - v(\omega - \varepsilon_\omega)]\cos\psi \tag{11}$$

If ψ is identically null (the vehicle is travelling parallel to the lane marking) then $\dot{\psi} = 0$ and we have $\varepsilon_\omega = \omega$, the gyro bias is then observable. Moreover, in this case, we have $\dot{C}_0$ is identically null so that one can observe that ψ is identically null.

Now, suppose that ψ is non null. By (10), we can work out:

$$\varepsilon_\omega = \frac{v \cdot \sin\psi - \dot{C}_0 \cdot \cos\psi}{C_0 \cdot \sin\psi} + \omega \tag{12}$$

C_0 is physically non null because the lane markings are on the sides of the lane.

By plugging (12) into (11), one gets a non-singular expression when the vehicle linear or rotational speeds are not null or when the vehicle accelerates or decelerates:

$$\left(\dot{v} \cdot C_0 - 3v \cdot \dot{C}_0 + \dot{\omega} \cdot {C_0}^2\right)\sin^3\psi - \left(3{\dot{C}_0}^2 - \ddot{C}_0 \cdot C_0\right)\cos^3\psi - \left(2{\dot{C}_0}^2 - \ddot{C}_0 \cdot C_0\right)\cos\psi + v \cdot \dot{C}_0 \cdot \sin\psi = 0 \tag{13}$$

From (13), there exists an implicit function Φ_ψ of C_0, $\dot{C}_0$, $\ddot{C}_0$, v, $\dot{v}$, ω and $\dot{\omega}$ such that:

$$\psi = \Phi_\psi(C_0, \dot{C}_0, \ddot{C}_0, v, \dot{v}, \omega, \dot{\omega}) \tag{14}$$

ψ is therefore observable.

By using (14) in (12), a function $\Phi_{\varepsilon_\omega}$ can give ε_ω:

$$\varepsilon_\omega = \Phi_{\varepsilon_\omega}(C_0, \dot{C}_0, \ddot{C}_0, v, \dot{v}, \omega, \dot{\omega}) \tag{15}$$

ε_ω is therefore observable.

3.2 Observability of the vehicle position (x, y) and GPS errors $(\varepsilon_x, \varepsilon_y)$

By taking the derivative of (8), we have:

$$\dot{x}_{GPS} = v \cdot \cos\psi - \varepsilon_x/\tau_x \tag{16}$$

So we can get:

$$\varepsilon_x = \tau_x(v \cdot \cos\psi - \dot{x}_{GPS}) \tag{17}$$

Since ψ is observable, ε_x is observable. So $x = x_{GPS} - \varepsilon_x$ is observable.

With $y = C_0 \cdot \cos\psi$ and (14), y is observable. With $\varepsilon_y = y_{GPS} - C_0 \cdot \cos\psi$, ε_y is observable.

So far, we have proved that every element in the state vector X can be expressed as an algebraic function of the components of $[Y, U]$ and a finite number of their derivatives. We can consequently conclude that the state vector with its associated state space is observable as long as the vehicle moves.

A positioning solver based on extended Kalman filtering with measured input has been developed and implemented in the local ENU frame. The location of the camera in the body frame is taken into account to get an accurate correction, please refer to [12] for more details about the EKF filter with measured input, the map matching method and the complete camera observation model. Outdoor experimental results are given in section 4.

4 RESULTS

4.1 Experimental set-up

Outdoor experiments have been carried out near Paris France in May 2013. Three tests were performed. Every test went on about 5 minutes, and the travelling distance was 3 km with a typical speed of 30 km/h in the straight road. The vehicle passed through a strong urban canyon with 300 meters' length. The experimental vehicle was equipped with an IMU Oxford RT3000 which provides ground truth data at 100Hz rate. A CAN-bus gateway was used to access to the wheel speed sensors and the yaw rate gyro. A Mobileye camera was used to detect the lane markings at 10Hz. A low-cost U-blox 6T GPS receiver with a patch antenna provided position measurements at 5Hz.

4.2 Localization results

The localization performance is studied by using a data replay processing implemented in C++ (identical to the software used in real-time) on different sequences than the ones used for AR parameters identification. Fig. 6a shows the test scene in the local ENU frame. The grey bounds represent buildings which are from OpenStreetMap to illustrate the urban condition of the test scene. The black lines represent the lane marking map expressed by polylines. The test scene mainly consists of two-lane roadways with dashed lane marking in the centre of the road and solid ones on both sides of the road. The map reaches a few-centimetres-level accuracy with often a better accuracy. The red line stands for the ground truth of the test trajectory of test 1. Fig. 6b shows changes of lateral and longitudinal positioning errors over time with $\pm 3\sigma$ bounds of test 1 estimated by the extended Kalman filter. One can notice that the uncertainty on lateral position increases greatly when lane marking measurements are not detected (in practice it remains often acceptable for autonomous navigation since this occurs mainly at roads intersections). The filter yields a better consistence on lateral positioning.

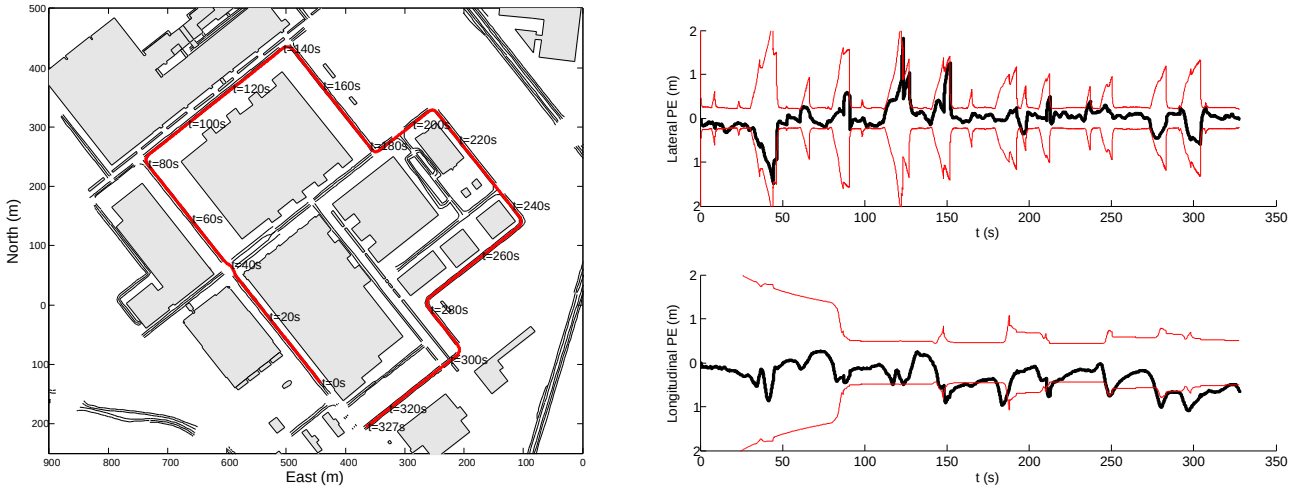

(a) Test scene (b) Map-aided positioning errors

Fig. 6. Test scene and Map-aided lateral and longitudinal positioning errors

	Lateral PE (m)		Longitudinal PE (m)	
	I	II	I	II
mean	1.30	0.07	1.55	-0.32
Std. dev.	1.12	0.29	1.18	0.32
median	0.96	0.10	1.31	0.30
95th percentile	3.20	0.68	3.88	0.88
max	6.78	1.83	4.69	1.50

Table 1. Positioning error statistics. (I: Stand-alone U-blox; II: Map-aided positioning)

Table 1 gives the global performance of three tests by stand-alone U-blox and Map-aided positioning. By using map-aided positioning, 95% lateral positioning errors (PE) are less than 0.68m and 95% and the longitudinal ones are less than 0.88m.

Fig. 7 compares the cumulative distributions of the absolute positioning errors. The localization accuracy is highly improved by map-aided positioning on both lateral and longitudinal directions.

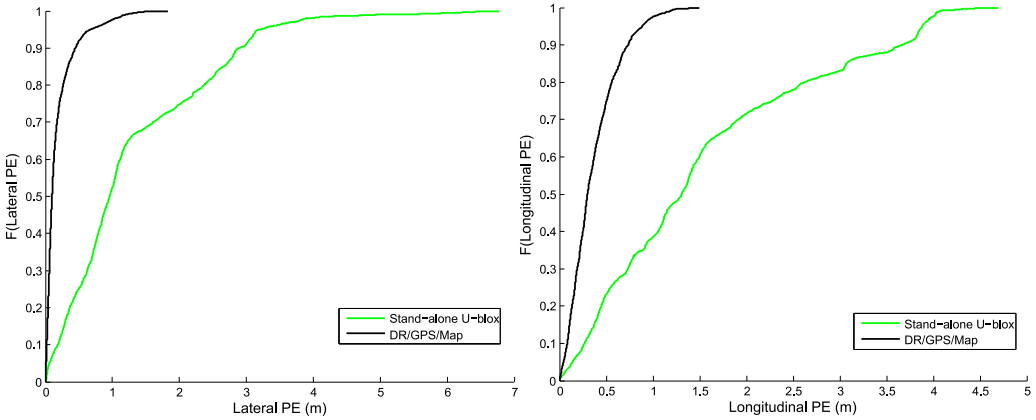

Fig. 7. Cumulative distribution function of the positioning errors

5 CONCLUSIONS

In this paper, we have first proposed an identification method of autoregressive parameters of shaping models of GPS errors. As shown, the GPS errors are well modeled by first order AR processes. This modelling keeps a complete observability of the augmented state vector when the vehicle is moving, which has been demonstrated according to an algebraic definition. A localization solver has been implemented in a local ENU frame to validate the proposed method with real outdoor data. The positioning accuracy is highly improved compared to stand-alone GPS. It is interesting to point out that ε_y is directly observable if the road is East oriented, which means that it is possible to use a more refined model to estimate ε_y. A perspective of this research is so to study if an implementation of the localization solver can be done in a road frame changing from one road to another in a sequential way.

Acknowledgements

The authors would like to thank Vincent Frémont, Stéphane Bonnet and Javier-Ibañez Guzman for their support in the experiments.

References

[1] J. Laneurit, R. Chapuis, and F. Chausse, "*Accurate vehicle positioning on a numerical map*," *International Journal of Control, Automation, and Systems*, vol. 3, no, 1, pp. 15-31, March 2006.

[2] I. Miller, M. Campbell, and D. Huttenlocher, "*Map-aided localization in sparse global positioning system environment using vision and particle filtering*," *Journal of Field Robotics*, vol. 28, no. 5, pp. 619-643, 2011.

[3] K. Jo, K. Chu, and M. Sunwoo, "*GPS-bias correction for precise localization of autonomous vehicles*," *Int. Vehicle Symp.*, pp. 636-641, 2013.

[4] Z. Tao, P. Bonnifait, V. Frémont, and J. Ibanez-Guzman, "*Mapping and localization using GPS, lane markings and proprioceptive sensors*," *IEEE Conf. on Int. Robots and Systems*, pp. 406-412, 2013.

[5] S. Nassar, "*Improving the inertial navigation system (INS) error model for INS and INS/DGPS Applications*," PhD thesis, University of Calgary, 2013.

[6] L. B. Jackson, "*Digital Filters and Signal Processing*," Kluwer Academic Publishers, 1996.

[7] J. Burg, "*Maximum entropy spectral analysis*," Stanford Exploration project. Stanford University, 1975.

[8] Y. Bar-shalom, X.-R. Li, and T. Kirubarajan, "*Estimation with Applications to Tracking and Navigation*," New York, NY, USA: John Wiley & Sons, Inc., 2002.

[9] H. Sert, W. Perruquetti, A. Kokosy, X. Jin, and J. Palos, "*Localizability of unicycle mobiles robots: An algebraic point of view*," *IEEE Conf. on Int. Robots and Systems*, pp. 223-228, 2012.

[10] R. Hermann and A. J. Krener, "*Nonlinear controllability and observability*," *IEEE Transactions on Automatic Control*, vol. 22, no. 5, pp. 728-740, Oct 1977.

[11] S. Wijesoma, K. W. Lee, and J. Ibanez-Guzman, "*On the observability of path constrained vehicle localization*," *IEEE Conf. on Int. Transp. Systems*, pp. 223-228, 2006.

[12] Z. Tao, P. Bonnifait, V. Frémont, and J. Ibanez-Guzman, "*Tightly coupling GPS with lane markings for autonomous vehicle navigation*," *IEEE 17th International Conf. on Int. Transp. Systems*, pp. 439-444, 2014.